Available online at www.sciencedirect.com
SCIENCE DIRECT
ELSEVIER
Nuclear Instruments and Methods in Physics Research A 527 (2004) 134–139
NUCLEAR INSTRUMENTS & METHODS IN PHYSICS RESEARCH
Section A
www.elsevier.com/locate/nima

Crystal and collimator optimization studies of a high-resolution γ-camera based on a position sensitive photomultiplier

N. Giokaris[a,b,*], G. Loudos[a], D. Maintas[a], A. Karabarbounis[a,b], V. Spanoudaki[a,b], E. Stiliaris[a,b], S. Boukis[a,b], A. Gektin[c], A. Boyarintsev[c], V. Pedash[c], V. Gayshan[d]

[a] Institute of Accelerating Systems and Applications, P.O. Box 17214, Athens 10024, Greece
[b] Physics Department, National Capodistrian University of Athens, Greece
[c] Institute for Scintillation Materials, Lenin Av. 60, Kharkov 310072, Ukraine
[d] Scintitech, 275 Concord Road, Wayland, MA 01778, USA

Abstract

Studies have been performed in order to optimize the collimator and the crystal of a γ-camera based on a position sensitive photomultiplier with respect its efficiency, its spatial resolution and its cost. Several parallel hole collimators of different thicknesses have been tested and compared to each other. The homogeneous crystals' performance has also been compared to that of a pixelized CsI(Tl) crystal. It is shown that though the spatial resolution of the homogeneous crystals is not as good as that of the pixelized one it is still reasonable and it could probably be improved by the choice of a better position reconstruction algorithm.

PACS: 87.58.Ce; 87.58.Pm; 87.57.Ce

Keywords: γ-Camera; Collimator; Crystal; Resolution; Efficiency

1. Introduction

Small field of view (FOV) high-resolution γ-cameras based on position sensitive photomultipliers (PSPMTs) have been used widely for studies with small animals and the development of new radiopharmaceuticals [1–5]. In the last few years several groups have demonstrated the ability of using such cameras for the early detection of small breast lesions in clinical applications and/or in experiments with phantoms [6–9].

The main components of such γ-cameras are the PSPMT, the collimator and the crystal and their choice in the end determines its main parameters which are the spatial resolution, the efficiency in γ-ray detection and the cost.

In this paper we describe the first part of a program which is still unfolding and whose purpose is to explore the possibility of building a γ-camera which has higher efficiency, good

*Corresponding author. IASA, P.O. Box 17214, Athens 10024, Greece. Tel.: +30-1-7257533; fax: +30-210-7295069.
E-mail address: ngiokar@cc.uoa.gr (N. Giokaris).

0168-9002/$ - see front matter
doi:10.1016/j.nima.2004.03.110

resolution and still costs less than our base design by the appropriate choice of its collimator and mainly its crystal. In Section 2 the main design of the γ-camera and the whole experimental setup are described. In Sections 3 and 4 the results of the studies with different collimators and crystals respectively are given. In Section 5 the conclusions from these studies are drawn.

2. Experimental setup

The gamma camera in its standard design consists of a PSPMT (Hamamatsu R2486), a parallel hole collimator and a pixilated CsI(Tl) scintillator. The thickness of the collimator is 2.75 cm, the holes are hexagonal $\sim$1.1 mm in diameter, with a 0.25 mm septa. The crystal is 4.6 cm in diameter, 3 mm thick and the cells' size is $1.13 \times 1.13\,\mathrm{mm}^2$ with 0.25 mm septa. The 16 anode signals are preamplified through 16 preamplifiers (LeCroy TRA1000) and then transferred to a CAMAC system, which hosts an ADC (LeCroy FERA 4300B), a memory (LeCroy FERA 4302), a driver (LeCroy FERA 4301) and a controller (Jorway 73A). The digital signals are transported to a G3 Power Mac via a SCSI bus. Acquisition software is written in Kmax 6.4.5. (Sparrow Corporation) environment. Details about the system and its readout principles can be found elsewhere [10].

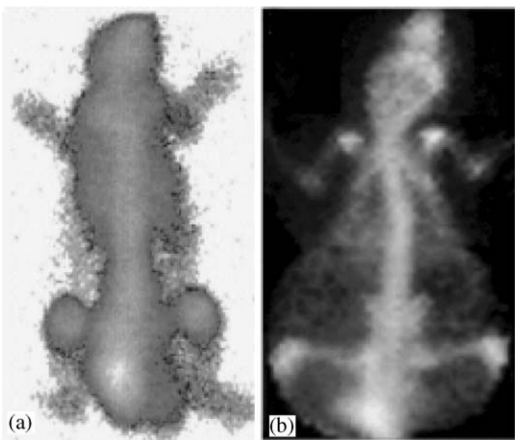

Fig. 1. A mouse injected with ^{99m}Tc-MDP, imaged with (a) an ECAT, Siemens gamma camera and (b) the same mouse imaged with the used PSPMT system.

The spatial resolution of the system has been measured and found <2 mm in planar imaging and 2 mm in SPECT mode [4,10]. This detector has been successfully used in small animal imaging and recently in imaging of breast phantoms [9]. In Fig. 1 the image of a small mouse injected with ^{99m}Tc-MDP is shown.

3. Collimator optimization studies

Three lead collimators have been tried. Their parameters are given in Table 1.

The standard CsI(Tl) pixelized crystal was used. The system's spatial resolution for 2D images was measured by using a thin (1.1 mm inner diameter) capillary filled with a ^{99m}Tc solution and placed at several distances from the collimator. The images FWHM versus the capillary–collimator distance is shown in Fig. 2.

Table 1
The parameters of the three collimators

#	Name	Hole shape	Hole diameter (mm)	Collimator thickness (mm)	Septum (mm)
1	Thin	Hexagonal	0.75	12	0.25
2	Standard	Hexagonal	1.12	27.5	0.25
3	Big	Circular	2	30	

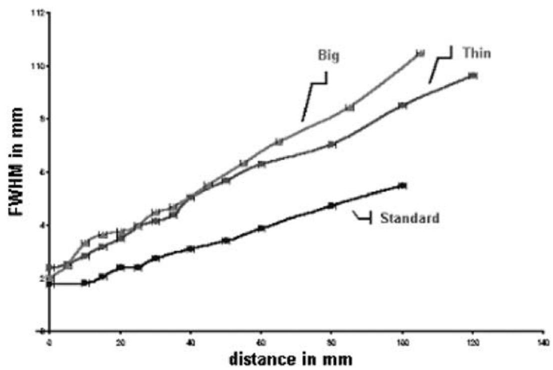

Fig. 2. The images FWHM versus the capillary–collimator distance for the three collimators.

The resolutions of the "big" and the "thin" collimators are virtually the same in the 0–10 cm distance range. The resolution of the "standard" is slightly better at small distances (0–120 mm) and significantly better for larger distances. It is clear that the "big" or the "thin" collimators could be used in cases where optimum resolution is not crucial but instead, high efficiency is desirable.

4. Crystal optimization studies

Five CsI(Tl) homogeneous crystals with 1, 2, 3, 5 and 7 mm thicknesses and 5 cm in diameter, all produced by "Institute for Scintillation Materials" were compared with the "standard" CsI(Tl) pixelized scintillator. In Fig. 3 the energy spectra of the five homogeneous crystals is shown as well as that of the pixelized one. A point ^{99m}Tc (140 keV) source was used in all cases.

The corresponding resolutions (FWHM of the photoelectric peak) are listed in Table 2.

It is seen that in all cases the resolution of the homogeneous crystals is, as expected, better than the pixelized one.

The images of a point source positioned in the middle of the FOV and close to the collimator for the 3 mm homogeneous crystal and the pixelized are shown in Fig. 4.

The center of gravity (COG) algorithm that has been found to work well for the pixelized crystal [1–10] was used. An obvious expansion of the source dimensions is produced by the homogeneous crystal. This is as result of the use of the COG algorithm and the fact that the produced light is not concentrated in a small surface, as in the case of the pixelized crystal, but spreads over almost the full crystal surface. This leads to a rather flat wire signal distribution for the homogeneous crystal as shown in Fig. 5.

Similar wire signal distributions but with the source now at the edges of the detector are shown in Fig. 6.

Here the use of the COG algorithm will have as a result points at the edge of the detector to be pulled towards the center. This is clearly seen in Fig. 7, where the image of a capillary before any

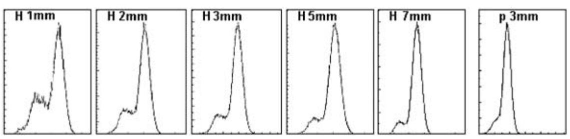

Fig. 3. Typical energy spectra of the five homogeneous crystals and the 3 mm pixelized one. (The scale of the energy spectrum of the pixelized crystal is not the same.)

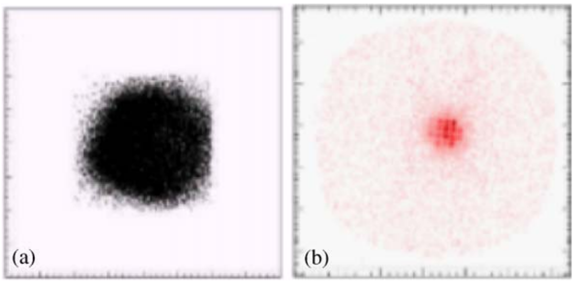

Fig. 4. The images of a point source in the middle of the FOV (a) for the 3 mm homogeneous crystal and (b) for the pixelized one.

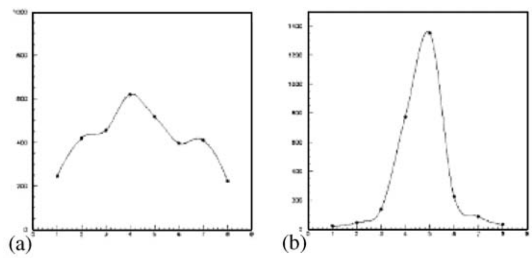

Fig. 5. Typical signal distributions (a) for the 3 mm homogeneous crystal and (b) the pixelized one. The source was placed in the middle of the FOV.

Table 2
Comparison of the energy resolution of the homogeneous with the pixelized crystal

Crystal	Hom. 1 mm	Hom. 2 mm	Hom. 3 mm	Hom. 5 mm	Hom. 7 mm	Pixel. 3 mm
Energy resolution (%)	19.4	21.2	21	23.4	23.5	26.7

corrections and after corrections to take care of the wire different responses and lower thresholds on the wire signals have been applied.

The homogeneous' crystals spatial resolution as a function of the object-collimator distance has been measured by using a thin (1.1 mm i.d.) capillary filled with a ^{99m}Tc water solution and is shown in Fig. 8. Only wires carrying more than 50% of the maximum wire signal were used for the estimation of the position by the COG algorithm.

It is seen that the best resolution of about 4.5 mm is obtained by the thinnest crystal and corresponds to small object-collimator distance as expected. The images of two capillaries, filled with a ^{99m}Tc solution, placed at different distances and the corresponding line profiles obtained by the 2 mm homogeneous crystal are shown in Fig. 9.

It is seen that the two capillaries can be resolved when their distance is larger than about 4.5 mm. In Fig. 10 the sensitivity versus the homogeneous crystal thichkness is shown.

The sensitivity seems to peak at a crystal thickness of 5 mm where the number of interacting primary gammas in the crystal and absorption of the secondary optical photons seem to be at the best balance.

In Fig. 11 the sensitivity of the pixelized crystal is compared with that of the thinner (1, 2 and 3 mm thickness) homogeneous crystals and is found to be slightly ($\sim$25%) lower than the one corresponding to the equal thickness homogeneous one.

5. Conclusions

This study has shown that using collimators with bigger holes and homogeneous instead of pixelized crystals does result in deterioration of the

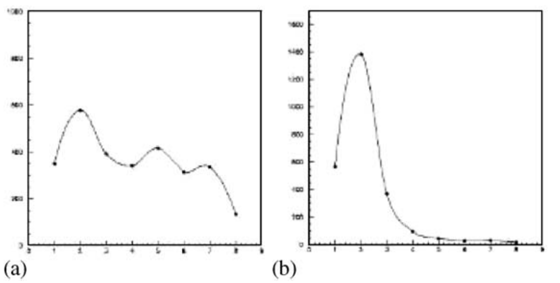

Fig. 6. Typical signal distributions (a) for the 3 mm homogeneous crystal and (b) the pixelized one. The source was placed at the edge of the detector.

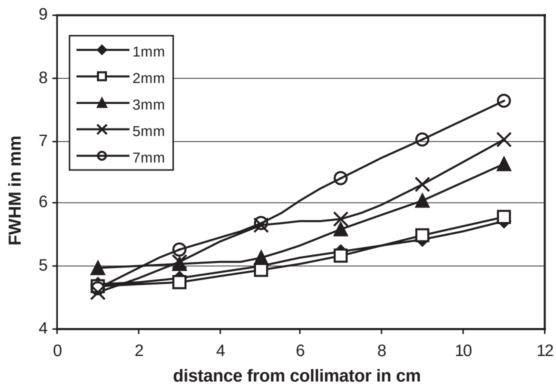

Fig. 8. The resolution versus the object-collimator distance for the five homogeneous crystals.

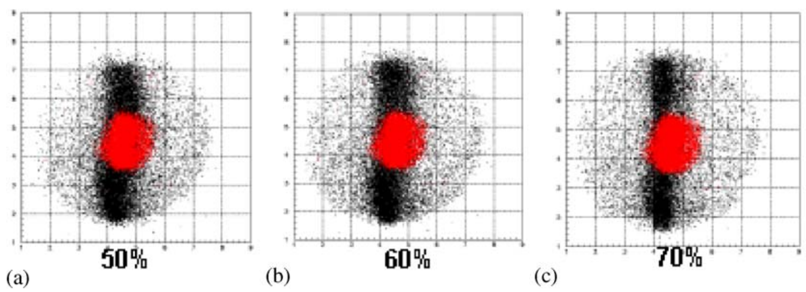

Fig. 7. The image of the capillary obtained with the 3 mm homogeneous crystal before any corrections (gray) and after (black) the applied corrections. Lower thresholds on wire signals are (a) 50%, (b) 60% and (c) 70%.

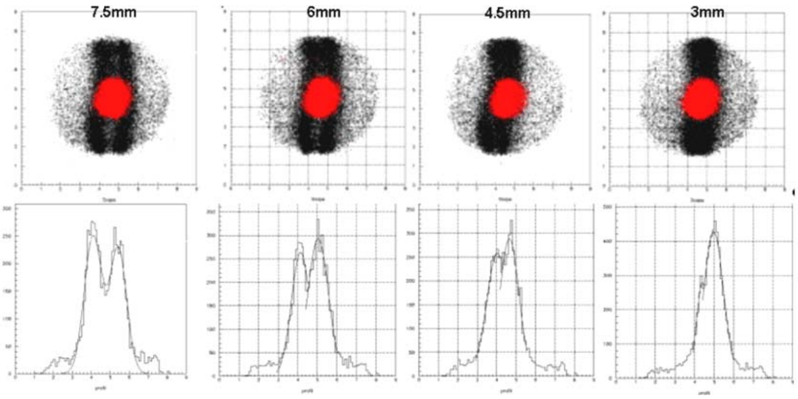

Fig. 9. Images and line profiles of two capillaries placed at 7.5, 6, 4.5 and 3 mm distances from each other. The 2 mm homogeneous crystal was used.

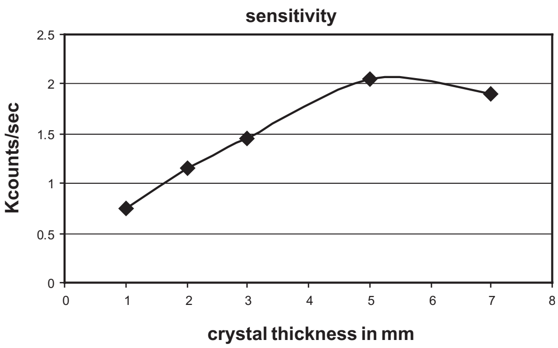

Fig. 10. Sensitivity versus crystal thickness.

spatial resolution though the effect is not large for small object-collimator distances.

However in cases where optimum resolution is not required and cost optimization is desired one can build a modest resolution system with a collimator with big holes and a few millimeter thick homogeneous crystal. This system will also have better energy resolution, higher efficiency and it will be also much easier to operate since one will not have to fight with the pixel to pixel non-uniformities encountered in a pixelized crystal system.

This situation could be further improved by the development of a better than the COG and more nicely adjusted to a homogeneous crystal, algorithm. Another approach to keep the cost low and still have resolutions comparable to those obtained

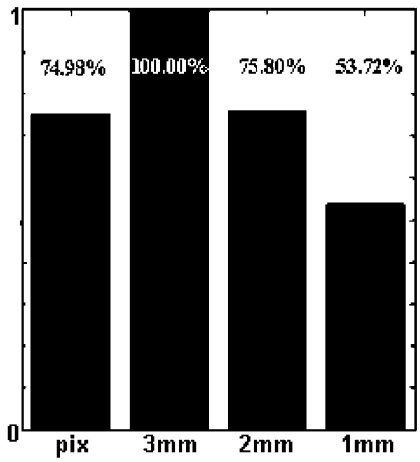

Fig. 11. Relative sensitivities of the 3 mm pixelized crystal and the 3, 2, and 1 mm thick homogeneous ones.

by the pixelized crystal, perhaps, to use of partially slotted [11] crystals which are now being evaluated by our group.

Acknowledgements

This work has been partly supported by the Greek General Secretariat for Research and Technology (GGET), by EEC RTN contract HPRN-CT-00292-2002 and by the Ministry of Education and Science of Ukraine, award

2M/182-2001. The authors would like to thank S. Majewski and A. Weisenberger of "Jefferson's lab" and R. Pani and F. Scopinaro of University of Rome "La Sapienza" for offering part of the used equipment.

References

[1] A.G. Weisenberger, E. Bradley, S. Majewski, M. Saha, IEEE Trans. Nucl. Sci. NS-l45 (3) (1998) 1743.
[2] N. Schramm, A. Wirrwar, H. Halling, IEEE Trans. Nucl. Sci. NS-47 (3)(Part 3) (2000) 1163
[3] J.H. Kim, Y. Choi, K.S. Joo, B.S. Sihn, J.W. Chong, S.E. Kim, K.H. Lee, Y.S. Choe, B.T. Kim, Phys. Med. Biol. 45 (11) (2000) 3481.
[4] G.K. Loudos, K.S. Nikita, N.D. Giokaris, E. Styliaris, S.C. Archimandritis, A.D. Varvarigou, C.N. Papanicolas, S. Majewski, D. Weisenberger, R. Pani, F. Scopinaro, N.K. Uzunoglu, D. Maintas, K. Stefanis, Appl. Radiat. Isot. 58 (4) (2003) 501.
[5] R. Pani, R. Pellegrini, A. Soluri, G. De Vincentis, R. Scafe, A. Pergola, Nucl. Instr. and Meth. A 409 (1–3) (1998) 524.
[6] R. Pani, R. Pellegrini, F. Scopinaro, et al., Nucl. Instr. and Meth. A 392 (1987) 295.
[7] A. Weisenberger, M. Williams, R. Wojcik, S. Majewski, F. Farzanpay, A. Goode, B. Kross, D. Steinbach, Nucl. Instr. and Meth. A 409 (1998) 520.
[8] S. Majewski, E. Curran, C. Keppel, D. Kieper, B. Kross, A. Pulumbo, V. Popov, A.G. Weisenberger, B. Welch, R. Wojcik, M.B. Williams, A.R. Goode, M. More, G. Zang, IEEE Trans. Nucl. Sci. NS-48 (3) (2001) 822.
[9] N.D. Giokaris, G.K. Loudos, D. Maintas, D. Papapanagiotou, K.S. Nikita, N.K. Uzunoglu, A. Karabarbounis, C.N. Papanicolas, E. Stiliaris, S.C. Archimandritis, A.D. Varvarigou, C.N. Stefanis, S. Majewski, R. Pani, F. Scopinaro, Nucl. Instr. and Meth. A 497 (1) (2003) 141.
[10] G.K. Loudos, K.S. Nikita, N.K. Uzunoglu, N.D. Giokaris, C.N. Papanicolas, S.C. Archimandritis, A.D. Varvarigou, D. Maintas, Comput. Med. Imaging Graphics 27 (4) (2003) 307.
[11] Gektin, V. Gavryluk, A. Boyarintsev, V. Gayshan, Second ITBS Conference, Milos, 26–30 May 2003.